

## Mechanistic Approach to the Flotation of Pure Pyrite

Eduardo Humeres \*, Nito A. Debacher, Newton L. Dias Filho,  
Maria M. de S. Sierra.

*Departamento de Química, Universidade Federal de Santa Catarina,  
88049 Florianópolis, SC, Brasil*

and

**Gaspar Gonzalez**

*Centro de Pesquisas da Petrobrás - CENPES, Ilha do Fundão,  
Quadra 7, Rio de Janeiro, RJ, Brasil*

Received: august 12, 1991

Um estudo cinético da flotação descontínua da pirita a 25°C, na ausência de espumantes, foi realizado num tubo de Hallimond modificado, com agitação mecânica (710 rpm). O tamanho das partículas estava na faixa de 420 - 590  $\mu\text{m}$  à 53 - 105  $\mu\text{m}$ . A constante velocidade observada é de primeira ordem com respeito ao número de partículas, mostra uma dependência de terceira ordem da concentração de bolhas e depende exponencialmente do diâmetro médio de partículas. O perfil de pH do logaritmo das constantes de velocidade (extrapoladas a concentração zero de tampão) mostra um máximo a pH 7. Nas condições deste estudo, cada partícula sofre uma rápida seqüência de colisões "pegajosas" formando um agregado final que contém uma média de três bolhas e que está em equilíbrio com outros agregados.

A kinetic study of the discontinuous flotation of pyrite at 25°C, in the absence of frother, was carried out in a modified Hallimond tube, with mechanical stirring (710 rpm). The particle size was in the range of 420 - 590  $\mu\text{m}$  to 53 - 105  $\mu\text{m}$ . The observed constant rate is first order with respect to the number of particles, shows a third order dependence on the bubble concentration and depends exponentially on the mean diameter of the particles. The pH profile of the logarithm of the rate constants (extrapolated to zero buffer concentration), shows a maximum at pH 7. Under the conditions of this study, each particle undergoes a rapid sequence of "sticky" collisions with bubbles, forming a final aggregate containing an average of three bubbles, forming a final aggregate containing an average of three bubbles, which is in equilibrium with other aggregates.

**Key words:** *flotation; pyrite.*

### Introduction

The presence of sulphur in coal produces pollution problems caused by the combustion products and has negative effects on the quality of the steel when used for metallurgical purposes. An important part of the sulphur in coals occurs as pyrite, whose removal is initially achieved using gravimetric separation procedures. However, selective flotation is considered, at present, to be one of the most promising techniques for coal desulphurization, particularly in the case of fine coal particles<sup>1</sup>.

There are several studies on the flotation of pyrite and other sulphides, in particular with respect to their native floatability and the mechanism of the heterogeneous reactions taking place at the mineral-solution interface when xanthate collectors (or other organic sulfur compounds) are used in flotation<sup>2-6</sup>. Studies of the kinetic aspects of flotation in systems are less numerous, and most deal with model systems. Moreover, the experimental approach is often oriented toward the specific dependence of the rate of flotation on the various phenomena associated to it<sup>7</sup>.

Studies on the rate of capture of particles by air bubbles have been restricted mainly to fine particles that are free of inertial forces and are much smaller than the bubbles. In this case flotation rate are in good agreement with the theoretically calculated collision rates<sup>8,9</sup>. The flotation rate of these particles increases with the particle diameter raised to the power 1.5 to 2.0 and decreases with the third power of the bubble diameter<sup>10-13</sup>. Flotability of very fine particles is slow relative to that of the other sizes, mainly due to the lower probability of collision between the particle and air bubbles<sup>10,14-16</sup>. However, attempts to develop theoretical relationships between flotation rate and particle size have been unsuccessful. Other factors like the relative velocities of particles and bubbles<sup>14</sup> and their surfaces charges<sup>13,17</sup> are also important contributors to the rate of flotation. The charges are determined, at least in part, by the pH of the dispersion. The flotation rate often reaches a maximum when the particle-bubble aggregate has an essentially zero net charge<sup>13</sup>.

The fundamental processes of attachment of a large particle to an air bubble were studied by Schulze<sup>18</sup>. Sharp-edged particles ensure the rupture of the wetting films; however, when the acceleration of the particle-bubble complex exceeds a critical value, the particle will detach<sup>19</sup>.

The complexity of the flotation process has not yet permitted the development of a quantitative description of the overall rate data in terms of surface chemistry, although several attempts have been made<sup>8</sup>. In general, the analysis considers the phenomena that take place in the pulp separately from those taking place in froth. This approach, known as the two-phase model, becomes very cumbersome since fractions containing different particle sizes must be considered.

The objective of this work is to study the flotation of coarse particles of pure pyrite from a kinetic point of view, analyzing the phenomenon as if it were a chemical reaction. In essence, the flotation process depends on the formation of stable bubble-particle aggregates through effective collisions between gas bubbles and solid particles. The rate equation of such a process can be expressed by Eq. 1, where  $N_b$  and  $N_p$  are the instantaneous concentrations of

bubbles and particles, and  $m$  and  $n$  the respective orders of the kinetic process in these concentrations<sup>20</sup>.

$$-\frac{dN_p}{dt} = k N_b^m N_p^n \quad (1)$$

The order, in this case, indicates the number of elementary species involved in the rate determining step and should give an insight into the mechanism of the process. For a complex system of several components the flotation occurs as a competitive process, and the rate constant for each component will determine the efficiency of the separation.

The rate constant, as defined in Eq. 1, is a complex function that depends on experimentally measurable properties of the system, such as the intrinsic wettability of the solid, the probability of effective collisions forming stable particle-bubble aggregates, the relative velocity between particles and bubbles, their relative size and the surface charge at the interface involved in the process. Considering that there are very few data on collision processes under controlled turbulent conditions, we will focus this study on the dependence of the rate constants on parameters such as particle size, air flow and pH, that may help to interpret the experimental values of the rate constant. Moreover, it will be assumed that the rate constant contains functions involving only one variable, using the well know method of separation of variables, whose most conspicuous example is the resolution of the wave function of hydrogen atom.

In this article, we report the results of the kinetics of flotation of pyrite in the absence of collectors. In subsequent papers, we will apply this analysis to the flotation of coal and examine the effect of various amphiphiles on the flotation kinetics.

## Experimental

### Materials

All chemicals were analytical grade and were used without further purification. Electrolytes and buffer solutions were prepared using distilled deoxygenated water. The pH was determined with a Metrohm Herisau model E603

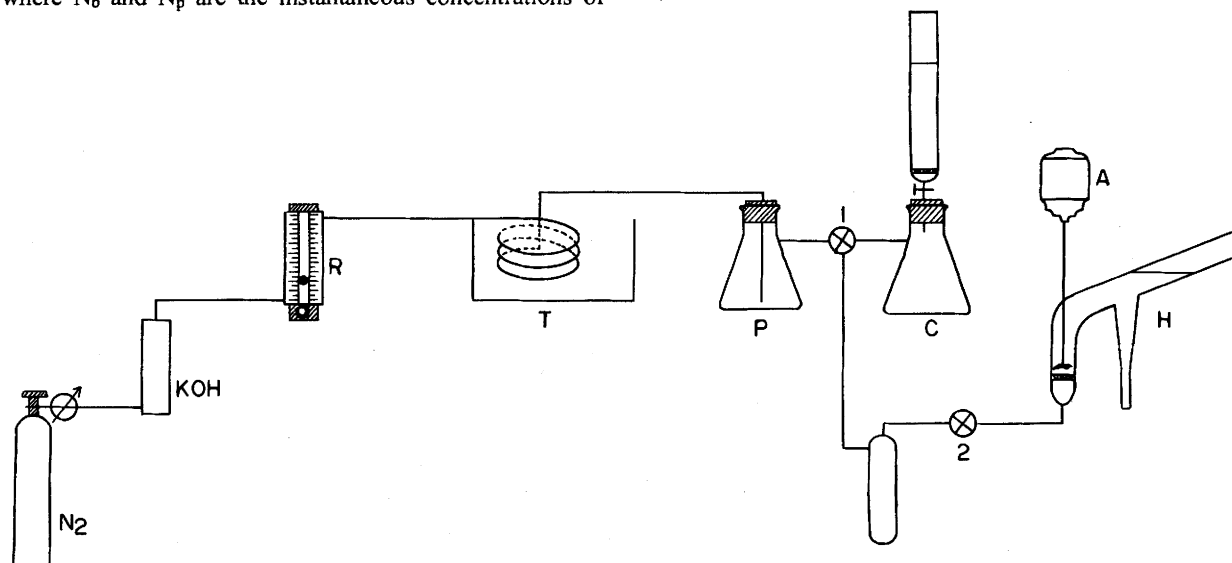


Figure 1. Scheme of the flotation system; R, flowmeter; T, thermostat; P, trap; C, pressure equalizer column; A, mechanical stirrer; H, modified Hallimond tube; B, collector tube.

pHmeter, using a Metrohm 9100 Herisau combination electrode.

Pyrite samples were selected from Carbonífera Próspera S.A., Mina A, Criciúma, in Santa Catarina State, and were kept in sealed plastic bags at  $-10^{\circ}\text{C}$ . The samples were reduced to about 5 mm size in a porcelain mortar and then pulverized in a Fritsch pulverizer and classified in a sieve shaker. The different fractions were stored in sealed bottles at  $-10^{\circ}\text{C}$ . The analysis by X - ray of the pyrite showed that it contained only traces of quartz.

#### Kinetics

In order to achieve reproducible results, the kinetic measurements were performed in a modified version of the Hallimond tube (H-tube) described by Fuerstenau *et al.*<sup>21</sup>. A mechanical stirrer controlled at 710 rpm was adapted through a ground glass joint to the sample compartment of the H-tube. The nitrogen, used as a carrier, passed through a column of KOH pellets, then through a calibrated flowmeter and a thermostat kept at  $25^{\circ}\text{C}$ , before entering the H-tube via a sintered glass plate. A pressure equalizer allowed the kinetic run to be started at the appropriate pressure. A schematic diagram of the setup is shown in Fig. 1.

The following procedure was adopted for each kinetic run. One gram of pyrite was washed several times with distilled water to eliminate fine material adhered to the mineral surface and spread over the porous sintered glass plate of the H-tube using a small volume of buffer solution. The upper part of the H-tube was then put in place and buffer solution added to complete 50 ml. The kinetics of the flotation process was followed by measuring the volume of mineral accumulated in the collector tube as a function of time. To ensure an homogeneous sedimentation and maximum packing of the floated particles, an ultravibrator was connected to the collector tube of the H-tube. The kinetics was found to be first order, according to the equation  $\ln(V_{\infty} - V_t) = kt$ , where  $V_{\infty}$  and  $V_t$  are the volumes of floated particles at time infinity and  $t$ , respectively. For each pH, the first order rate constants were determined at two buffer concentrations (10 and 50 mM) and extrapolated to zero buffer concentration. The first order rate plots were linear with correlation coefficients of at least 0.99 with standard deviation of about 10% in the value of the rate constant. Some typical examples at different pH are shown in Fig. 2. Experiments with particles of several sizes showed that half life is constant when the

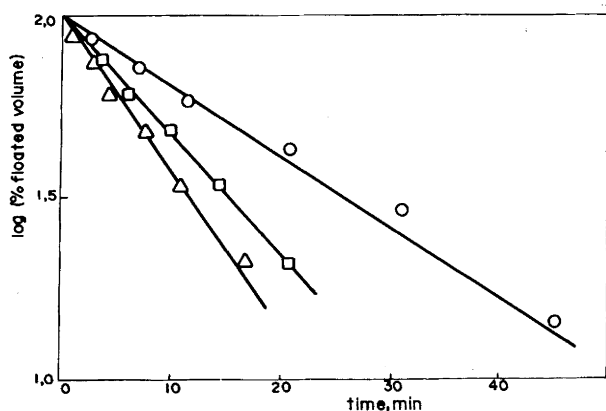


Figure 2. Plot of  $\log (\% \text{ floated volume})$  versus time at different pH's; at  $25^{\circ}\text{C}$ ; 50 mM buffer; particle size 210-297  $\mu\text{m}$ ; gas flow 1 l  $\text{min}^{-1}$ ; O, pH 3;  $\square$ , pH 6;  $\Delta$ , pH 7.

weight (or number of particles) was changed, as predicted for first order kinetics.

## Results and Discussion

According to Fig. 2, under the experimental conditions of this work, the batch flotation of pyrite follows first order kinetics with respect to the number of particles per unit of volume, as shown in Eq. 2. Similar results have been obtained for pyrite<sup>1</sup> and other particles<sup>12</sup> under other experimental conditions. Comparison of Eq.1 and 2 leads to  $n=1$ . The observed first order rate constant,  $k_{\text{obs}}$ , is undoubtedly a complex

$$-\frac{dN_p}{dt} = k_{\text{obs}} N_p \quad (2)$$

function; nonetheless, we will assume that  $k_{\text{obs}}$  may be represented as the product of separable functions and constants as in Eq. 3. The constant  $k_g$  depends on the geometry of the H-tube, mainly on the stirring and the porosity of the sintered glass plate, which determine the size of the bubbles. The constant  $k_i$  depends on intrinsic characteristics of the system such

$$k_{\text{obs}} = k_g k_i f_v f_D f_{\text{pH}} \quad (3)$$

as particles shape and the hydrophobicity of the particle surface;  $f_v$ ,  $f_D$  and  $f_{\text{pH}}$  are functions that depend only on the gas flow, particle size and the pH of the dispersion, respectively.

#### Effect of the gas flow

When nitrogen is injected into the H-tube at a flow rate  $V$ , through a sintered glass plate of a given porosity a number,  $n_b$ , of bubbles with an average volume  $\bar{v}_b$  are formed per unit time. The concentration of bubbles  $N_b$  rising through the flotation media will be given by:

$$N_b = \frac{V}{\bar{v}_b} \frac{\tau}{V_d} \quad (4)$$

where  $\tau$  is the average residence time of a bubble in the flotation system and  $V_d$  is the volume of the dispersion in which the particles are confined.

Two series of experiments were carried out with two different particle sizes, varying the gas flow in the range of 0.50 - 1.2 l/min.; the results are shown in Fig. 3. In both cases, the dependence of  $k_{\text{obs}}$  with respect to the gas flow, yielded linear plots of  $\log k_{\text{obs}}$  versus  $\log V$  with slopes equal to three (see insert in Fig. 3). Thus, in terms of Eq.1 and 3,  $f_v = V^3$  and the factor  $(\tau/\bar{v}_b \cdot V_d)^3$  is part of the constant  $k_g$  dependent on the geometry of the H-tube (Eq. 4). This result suggests that three bubbles are involved in the flotation of one pyrite

$$k_{\text{obs}} = k N_b^m = k_g k_i V^3 f_D f_{\text{pH}} \quad (5)$$

particle. With the present results, it is not possible to decide to what extent the bubbles coalesce during the capture process.

The chance of a simultaneous contact between a particle and three bubbles is virtually zero. The most attractive alternative is a sequence of "sticky" collisions<sup>22</sup>, forming aggregates whose lifetimes permit subsequent collisions to form the final aggregate  $\text{PB}_3$  that floats (Eq.5). The detachment of

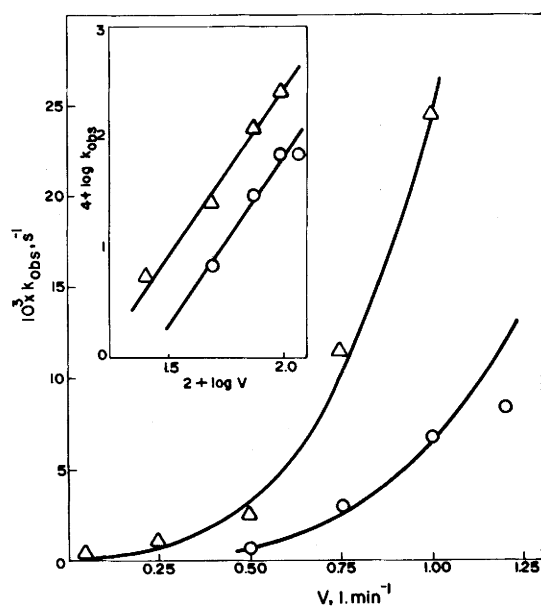
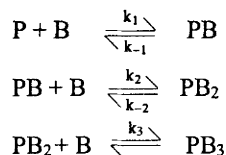


**Figure 3.** Plot  $k_{obs}$  versus gas flow;  $\Delta$ , at  $25^\circ\text{C}$ ; particle size  $53\text{-}105\ \mu\text{m}$ , pH 6 (succinate  $50\ \text{mM}$ );  $\text{O}$ , particle size  $149\text{-}210\ \mu\text{m}$ , pH 7 (phosphate  $50\ \text{mM}$ ). Curves were calculated according to Eq. 4. The two straight lines of the insert were drawn with slope 3.

aggregate PB to regenerate  $\text{P} + \text{B}$  is much faster than the collision with the second bubble, i.e.  $k_1(\text{PB}) > k_2(\text{PB})(\text{B})$ , and similarly  $k_2(\text{PB}_2) \gg k_3(\text{PB}_2)(\text{B})$ . Therefore, the aggregate  $\text{PB}_3$  is essentially in equilibrium with the other aggregates and is formed at a rate equal to  $k_3(\text{PB}_2)(\text{B})$ . In the case of trimolecular reactions, the experimental Arrhenius activation energies are very small and the



rate constants therefore, depend mainly on the collision number<sup>22</sup>.

Considering that the bubble concentration is constant during the experiment, the constant  $k_g$  should be inversely proportional to the cube of the average bubble volume  $\bar{v}_b$ . If only one bubble were needed, the flotation rate would decrease as the third power of the bubble diameter<sup>11,13</sup>; therefore, since three bubbles are needed to float one pyrite particle, the rate constant should depend on  $\bar{v}_b^{-3}$ . For both situations, reduction of the bubble size should rapidly increase the rate of flotation of pyrite.

#### Effect of particle size

This effect was studied in the range of particle size from  $420\text{-}590\ \mu\text{m}$  down to  $53\text{-}105\ \mu\text{m}$ . As shown in Fig. 4, for particles larger than  $100\ \mu\text{m}$  in diameter, the log of the rate constant decreases linearly with the mean particle diameter  $\bar{D}$ , in accord with Eq. 6, where  $a = -5.28$  and  $B = 13.27 \times 10^{-2}$ . From

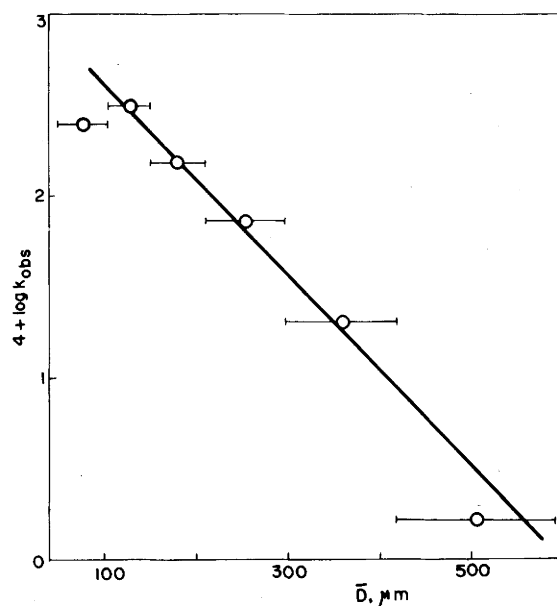


**Figure 4.** Plot of  $\log k_{obs}$  versus mean diameter of the particles; at  $25^\circ\text{C}$ ; gas flow  $1\ \text{l.min}^{-1}$ ; pH 6 (succinate  $50\ \text{mM}$ ).

$$\log k_{obs} = a\bar{D} + \log B \quad (6)$$

Eq. 3,  $f_D = 10^{a\bar{D}} = e^{b\bar{D}}$  where  $b = -12.16$  and  $k_{obs}$  can be written as Eq. 7.

$$k_{obs} = k_g k_i V^3 e^{-b\bar{D}} f_{pH} \quad (7)$$

From Fig. 4, the rate constant expected for particles of  $50\ \mu\text{m}$  diameter, should be about  $10^{-2}\text{s}^{-1}$ , which is of the same order of magnitude found for pyrite<sup>23</sup> and polystyrene<sup>12</sup> particles. Rate maxima for a range of particle size have been observed in a number of systems<sup>23</sup>, such as galena<sup>24</sup>, calcite<sup>20</sup>, and quartz<sup>25</sup>. Particles with diameters of  $100\text{-}500\ \mu\text{m}$  are in the common range found in many flotation processes. As the particle diameter increases, the probability of collision increases, but the particle/bubble aggregate becomes unstable because of inertial forces and the rate constant decreases<sup>18,20</sup>. We note that the expected dependence of the rate constant on particle diameter of the type  $\bar{D}^c$ <sup>10,12</sup>, where  $c = 1.5$  to  $2.0$ , is not applicable in this system; thus, for the relationship  $f = e^{b\bar{D}} = \bar{D}^c$  to hold,  $c$  would have to change from  $0.53$  to  $8.77$  in the range of  $\bar{D} = 100$  to  $500\ \mu\text{m}$ .

#### Effect of pH.

In order to study the effect of pH in the range of pH 2 - 12, appropriate buffers were used at two different concentrations ( $10$  and  $50\ \text{mM}$ ) and the rate constants extrapolated to zero buffer concentration.

Three series of experiments were carried out. In the first two series, pyrite samples with the same particle size ( $149\text{-}210\ \mu\text{m}$ ) were used and the plate porosity of the H-tube was changed. In the third series, the particle size was increased to  $210\text{-}297\ \mu\text{m}$ . Three bell shaped curves were obtained with a maximum at pH around 7 (Fig. 5). Normalization of the values of the rate constants obtained in each of the three

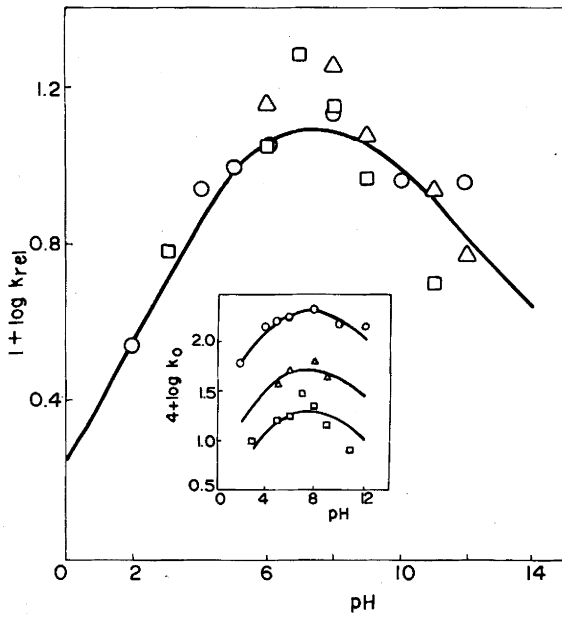


**Figure 5.** pH profile of the flotation of pyrite at 25°C. The rate constants were extrapolated to zero buffer concentration and divided by the corresponding value at pH 5 for each series of experiments; gas flow 1 l.min<sup>-1</sup>; O particle size 149-210 μm, porosity 1; Δ, particle size 149-210 μm, porosity 2; □, particle size 210-297 μm, porosity 2; ●,  $k_{rel} = 1$ .

series of experiments relative to the values at pH 5 ( $k_5$ , Eq.8) provides a single set of relative rate constants that depends only on  $f_{pH}$ , as shown in Fig. 5.

$$k_{rel} = \frac{k_{obs}}{k_5} = \frac{f_{pH}}{f_5} \quad (8)$$

According to Eq. 1 and 5, there are three bubbles and one particle involved in the process of forming the aggregate PB<sub>3</sub> that is capable of floating. Therefore, the function  $f_{pH}$  in Eq. 3 involves the net effect of pH on these four species, which is presumed to be similar to the pH dependence of the aggregate PB<sub>3</sub> itself. Many questions remain to be understood yet as the details of the processes that produce such an aggregate. As a first approximation, we will consider that a change of the concentration of protons in the bulk of the solution changes the electrokinetic potential of the whole bubble-particle aggregate<sup>7</sup>. The effect of the pH would be to modify the number of protons attached to the aggregate<sup>26</sup>.

We will consider a simple model in which, at a particular pH, the bubble-particle aggregate has  $n$  equivalent positively charged sites and  $m$  neutral sites. Equilibrium with the solution proceeds very rapidly and the sites do not interact with one another. In this model, the exchange or adsorption of other ions at the solid or bubble-solution interface of the aggregate is not considered. Therefore, from this point view, a neutral aggregate does not necessarily mean an aggregate with zero potential, but rather one with balanced proton charge. An aggregate with an excess of  $n$  protons is represented as  $A^n$ , and one with a deficiency of  $m$  protons is represented as  $A^m$  (positive or negative signs have been

omitted for simplicity). All aggregates are in equilibrium with the free protons of the dispersion, as shown in Eqs. 9.



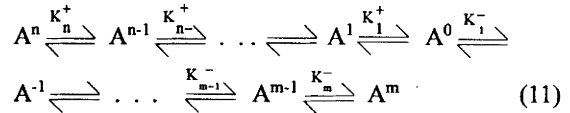
The equilibrium constants  $K_n^+$  and  $K_m^-$  can be expressed, in molar units, as Eqs. 10, where concentration of aggregates

$$K_n^+ = \frac{[A^{n-1}]}{[A^n]} \cdot a_H \quad (10a)$$

$$K_m^- = \frac{[A^m]}{[A^{m-1}]} \cdot a_H \quad (10b)$$

is given in number of aggregates per unit volume and  $a_H$  is the activity of protons in moles per litre.

Aggregates with different numbers of protons can be represented as a set of consecutive equilibria (Eq. 11).



At a particular pH, there will be a distribution of aggregates,  $A^i$  ( $i=n,m$ ), that behave similarly to the kinetic term  $\{N_b^3 N_p\}^i$  with respect to the pH. Therefore, the total rate of flotation will result from the sum of the individual rates  $v_i$  that depend on the values of  $n$  and  $m$  of ( $A^i$ ), as shown in Eq. 12 where the total aggregate concentration ( $A^i$ )<sub>tot</sub> is given by Eq. 13.

$$v_{tot} = \sum k_n [A^n] + \sum k_m [A^m] + k_0 [A^0] \quad (12)$$

$$[A^i]_{tot} = \sum [A^n] + \sum [A^m] + [A^0] \quad (13)$$

If it is assumed that all  $K_n^+$  are equal to  $K^+$  and all  $K_m^-$  are equal to  $K^-$ , the concentrations of all the aggregates with an excess of deficiency of protons will be given by Eqs. 14 and 15, respectively.

$$\sum [A^n] = \frac{\frac{a_H}{K^+} \{[A^0] - [A^n]\}}{1 - \frac{a_H}{K^+}} \quad (14)$$

$$\sum [A^m] = \frac{\frac{K^-}{a_H} \{[A^0] - [A^m]\}}{1 - \frac{K^-}{a_H}} \quad (15)$$

From the equilibrium expressions (Eqs. 10), Eq. 16 and 17 can be obtained. Substituting for ( $A^n$ ) and ( $A^m$ ) in Eq. 13 provides Eq. 18 in which the concentration of the neutral species

$$K_1^+ \cdot K_2^+ \dots K_n^+ = (K^+)^n = \frac{a_H^n [A^0]}{[A^n]} \quad (16)$$

$$K_1^- \cdot K_2^- \dots K_m^- = (K^-)^m = \frac{a_H^m [A^m]}{[A^0]} \quad (17)$$

Table 1. Kinetic Parameters for the Flotation of Pyrite.

Variable	Range	Constant functions <sup>a</sup>			
		$f_v$	$f_D$	$f_{pH}$	$10^2 k_g k_i, 1^{-3} s^{-1}$
V	0.05 - 1.0 l min <sup>-1</sup>	—	0.383	0.938	5.49 <sup>c</sup>
V	0.5 - 1.2 l min <sup>-1</sup>	—	0.112	0.985	5.39 <sup>c</sup>
D	53 - 590 μm	1	—	0.938	14.60 <sup>d</sup>
pH	2 - 12	1	0.112	—	19.60 <sup>d</sup>
pH	5 - 9	1	0.112	—	4.80 <sup>c</sup>
pH	3 - 11	1	0.048	—	4.22 <sup>c</sup>

a) Calculated according to Eqs. 7 and 22; b) average value; c) porosity 2; d) porosity 1.

(A<sup>0</sup>) is expressed in terms of the total concentration of aggregates at different pH's, where P<sub>n</sub> and Q<sub>m</sub> are functions of the maximum values of n and m (Eqs. 19). Therefore, k<sub>obs</sub> can be expressed in terms of Eq. 20.

$$[A^0] = \frac{[A]_{tot}}{P_n + Q_m + 1} \quad (18)$$

$$P_n = \frac{a_H}{K^+} \left[ \frac{1 - \left(\frac{a_H}{K^+}\right)^n}{1 - \frac{a_H}{K^+}} \right] \quad (19a)$$

$$Q_m = \frac{K^-}{a_H} \left[ \frac{1 - \left(\frac{K^-}{a_H}\right)^m}{1 - \frac{K^-}{a_H}} \right] \quad (19b)$$

$$k_{obs} = \frac{\sum k_n \left(\frac{a_H}{K^+}\right)^n + \sum k_m \left(\frac{K^-}{a_H}\right)^m + k_0}{P_n + Q_m + 1} \quad (20)$$

Fig. 5 indicates that, at low and high pH values, flotation becomes slow. Under these conditions, the aggregate should present a fairly high charge density. Consequently, aggregate presenting small or zero charge density would appear to float more efficiently. In this case, k<sub>n</sub> = k<sub>m</sub> = 0 and k<sub>obs</sub> is represented by Eq. 21, where k<sub>o</sub> = k<sub>g</sub>k<sub>i</sub>f<sub>D</sub>f<sub>v</sub> and f<sub>pH</sub> is given by Eq. 22.

$$k_{obs} = \frac{k_o}{P_n + Q_m + 1} \quad 21$$

$$f_{pH} = (P_n + Q_m + 1)^{-1} \quad 22$$

Eq. 21 was adjusted by a successive approximation program to the relative rates calculated according to Eq. 8. The best fit was obtained for pK<sup>+</sup> = 5.39, pK<sup>-</sup> = 8.88, n = 0.16 and m = 0.09 (Fig. 5). According to Eq. 20, n and m should be integers. The fact that the best fit values are less than one suggests that these are weighted values (between zero and one) and that there are only a few positive or neutral sites on the aggregate. The proximity of the value of pK<sup>+</sup> and pK<sup>-</sup> is consistent with the interpretation.

## Conclusion

Table 1 summarizes the range of the variables studied and the rate constants (k<sub>g</sub> k<sub>i</sub>) calculated over relatively wide conditions. The porosity of the two glass plates used in the experiments can be defined only as fine (porosity 1) and coarse (porosity 2). Accordingly, the values of k<sub>g</sub> change, the product (k<sub>g</sub> k<sub>i</sub>) being equal to 17.10 x 10<sup>-21-3</sup> s<sup>-1</sup> for porosity 1 and 4.98 x 10<sup>-21-3</sup> s<sup>-1</sup> for porosity 2. Therefore, within the limits studied, the rate constant for flotation of pyrite can be calculated with reasonable accuracy.

These results show that the rate constants of flotation can, in effect, be factored as assumed in Eq. 3. This approach should permit optimization of the separation of particles based on a consideration of the functions that are sensitive to each flotation parameter such as air flow, pH, particle diameter and bubble size.

## Acknowledgments

This research was supported by Financiadora de Estudos e Projetos (FINEP) and by the Conselho Nacional de Desenvolvimento Científico e Tecnológico (CNPq).

## References

1. F.F. Aplan, *Use of Flotation Process for Desulfurization of Coal, in Coal Desulfurization. Chemical and Physical Methods*, T.D. Wheelock, ed., (ACS Symposium Series, Washington, 1977).
2. A.V. Glemobtskii, L.Ya. Shubov and A.K. Livshits, *Tsvet. Metal.* **41**, 11-14 (1968).
3. M.C. Fuerstenau, J.L. Huiatt and M.C. Kuhn, *Trans. AIME* **250**, 227-31 (1971).
4. K.J. Miller, *Trans. AIME* **258**, 30-33 (1975).
5. M. Tsai, N. Takahashi and J. Shimouzaka, *Nippon Kogyo Kaishi* **87**, 533 - 7 (1971).
6. J.R. Gardner and R. Woods, *Aust. J. Chem.* **30**, 981-91 (1977).
7. H.J. Schulze, *Physicochemical Elementary Processes in Flotation* (Elsevier, Berlin, 1983).
8. K.J. Ives, *The scientific Basis of Flotation* (M. Nijhoff Publ., The Hague, 1984).
9. J.F. Anfruns and J.A. Kitchener, *Inst. Min. Met.*, c9 - c15 (1977).
10. D. Reay and G. A. Ratcliff, *Can. J. Chem. Eng.* **51**, 178-85 (1973).

11. D. Reay and G.A. Ratcliff, *Can. J. Chem. Eng.* **53**, 481-6 (1975).
12. G.L. Collins and G.L. Jameson, *Chem. Eng. Sci.* **31**, 985-91 (1976).
13. G.L. Collins and G.L. Jameson, *Chem. Eng. Sci.* **32**, 239-46 (1977).
14. K.L. Sutherland, *J. Phys. & Colloid Chem.* **52**, 394-425 (1948).
15. L.R. Flint and W.J. Howarth, *Chem. Eng. Sci.* **26**, 1155-68, (1971).
16. W.J. Trahar and L.J. Warren, *Int. J. Miner. Process.* **3**, 103-31 (1976).
17. H.J. Schulze and C. Cichos, *Z.Phys. Chem.* **251**, 252-68 (1972).
18. H.J. Schulze, *Int. J. Miner. Process.* **4**, 241 - 259 (1977).
19. A. Jowett in *Fine Particle Processing*, Proc. Int. Symp. on Fine Particles (Las Vegas, Nevada, 1980).
20. S.N. Tewari and A.K. Biswas, *J. Appl. Chem.* **19**, 173-7 (1969).
21. D.W. Fuerstenau, P.H. Metzger and G.D. Seale, *Eng. Min. J.* **158**, 93-5 (1957).
22. J.W. Moore and R.G. Pearson, *Kinetics and Mechanism* (Wiley, New York, 1981), ch. 4.
23. W.J. Trahar, *Int. J. Min. Process.* **8**, 289 - 327 (1981).
24. A.M. Gaudin, R. Schuhmann and A.W. Schlechten, *J. Phys. Chem.* **46**, 902-10 (1942).
25. P.L. de Bruyn and H.J. Modi, *Min. Eng.* **8**, 415-19 (1956).
26. D.J. Shaw, *Introduction to Colloid and Surface Science* (Butterworth, London, 1980).